3 Biotech (2021) 11:431
https://doi.org/10.1007/s13205-021-02976-5

ORIGINAL ARTICLE

Development of a real-time RT-PCR method for the detection of *Citrus tristeza* virus (CTV) and its implication in studying virus distribution in planta

Sunil B. Kokane[1,2] · Pragati Misra[2] · Amol D. Kokane[1] · Mrugendra G. Gubyad[1] · Ashish J. Warghane[1,3] · Datta Surwase[1] · M. Krishna Reddy[4] · Dilip Kumar Ghosh[1]

Received: 9 June 2021 / Accepted: 23 August 2021 / Published online: 11 September 2021

Abstract

Tristeza is an economically important disease of the citrus caused by *Citrus tristeza* virus (CTV) of genus *Closterovirus* and family Closteroviridae. The disease has caused tremendous losses to citrus industry worldwide by killing millions of trees, reducing the productivity and total production. Enormous efforts have been made in many countries to prevent the viral spread and the losses caused by the disease. To understand the reason behind this scenario, studies on virus distribution and tropism in the citrus plants are needed. Different diagnostic methods are available for early CTV detection but none of them is employed for *in planta* virus distribution study. In this study, a TaqMan RT-PCR-based method to detect and quantify CTV in different tissues of infected Mosambi plants (*Citrus sinensis*) has been standardized. The assay was very sensitive with the pathogen detection limit of > 0.0595 fg of in vitro-transcribed CTV-RNA. The assay was implemented for virus distribution study and absolute CTV titer quantification in samples taken from Tristeza-infected trees. The highest virus load was observed in the midribs of the symptomatic leaf (4.1×10^7–1.4×10^8/100 mg) and the lowest in partial dead twigs (1×10^3–1.7×10^4/100 mg), and shoot tip (2.3×10^3–4.5×10^3/100 mg). Interestingly, during the peak summer months, the highest CTV load was observed in the feeder roots (3×10^7–1.1×10^8/100 mg) than in the midribs of symptomatic leaf. The viral titer was highest in symptomatic leaf midrib followed by asymptomatic leaf midrib, feeder roots, twig bark, symptomatic leaf lamella, and asymptomatic leaf lamella. Overall, high CTV titer was primarily observed in the phloem containing tissues and low CTV titer in the other tissues. The information would help in selecting tissues with higher virus titer in disease surveillance that have implication in Tristeza management in citrus.

Keywords *Citrus tristeza* virus · *In planta* distribution study · TaqMan RT-PCR · CTV titer quantification

Introduction

Citrus is an important fruit crop in India, ranking third after mango and banana. The major biotic factors responsible for low citrus productivity include virus and virus-like pathogens viz., *Citrus tristeza virus* (CTV), *Citrus yellow mosaic virus* (CYMV), *Indian citrus ringspot virus* (ICRSV), Citrus greening (Huanglongbing, HLB), Citrus exocortis viroid (CEVd) and Citrus Phytoplasma (Ghosh et al. 2015, 2019; Kokane et al. 2020a, 2021a). Among these, Citrus tristeza caused by CTV had serious impact on citrus production worldwide and ranked as the most destructive citrus disease after Citrus greening. It has killed over hundreds of millions of citrus trees for the past 70 years and becomes a major threat to the global citrus industry (Dawson et al. 2013; Ghosh et al. 2020a). CTV has been disseminated

✉ Dilip Kumar Ghosh
ghoshdk@hotmail.com

1 Plant Virology Laboratory, ICAR-Central Citrus Research Institute, Nagpur, Maharashtra 440033, India

2 Department of Molecular and Cellular Engineering, Sam Higginbottom University of Agriculture, Technology and Sciences, Allahabad, Uttar Pradesh 211007, India

3 Faculty of Life Sciences, Mandsaur University, Mandsaur, MP 458001, India

4 ICAR-Indian Institute of Horticultural Research, Bangalore, Karnataka 560089, India

widely to almost all the citrus growing regions of India with prevalence of 47.1–56% in the Northeast region of India, 36–50% in the southern region of India, 26.3% in Vidarbha region of Maharashtra, and 16–60% in the North–Northwest region of India (Biswas et al. 2014; Warghane et al. 2019). CTV is a member of the genus *Closterovirus* of the family Closteroviridae. The virus has a monopartite single-stranded positive-sense RNA genome of ~19.3 kb that remains encapsidated in 2000 × 11 nm flexuous filamentous virions. The genome is divided into two parts that contain a total 12 open reading frames (ORFs), which encode at least 19 different proteins. The 5′ end of genome consists of ORF1a and 1b encoding proteins involved in viral replication and the 3′ end contains ten ORFs encoding proteins required for viral structure, virion assembly and host–vector interaction.

The major capsid protein (CP) and minor capsid protein (CPm) are encoded by p25 gene and p27 gene, respectively (Karasev et al. 1995; Albiach-marti et al. 2010; Ghosh et al. 2020a). Tristeza affects most of the citrus species/cultivars, hybrids, and causes a wide array of symptoms including stem pitting, stunting, vein clearing, vein flecking that result in either slow decline or rapid decline. Citrus decline has been occurred mostly in those countries where sour orange was used as predominant rootstock (Moreno et al. 2008; Ghosh et al. 2020b). In India, citrus decline was mostly observed in sweet oranges grafted on rough lemon or sweet orange rootstocks than the other citrus cultivars (Vasudeva et al. 1959; Ahlawat 1997). The disease spreads from infected to healthy trees through exchange of infected tissue for budding/grafting and by different aphid vectors like *Toxoptera citricida* Kirkaldy, *Aphis spiraecola* Patch and *Aphis gossypii* Glover in a semi-persistent manner (Marroquín et al. 2004).

Diagnostic methods employed for CTV detection include biological indexing, ELISA (enzyme-linked immunosorbent assay), dot-immuno-binding assay, electron microscopy, and reverse transcriptase-polymerase chain reaction (RT-PCR) (Bar-Joseph et al. 1989; Warghane et al. 2017a,b; Kokane et al. 2020b). Diagnosis of virus by conventional RT-PCR is the most reliable method (Kokane et al. 2020c). However, sometimes conventional RT-PCR may not detect pathogen due to low titer in the tissue. Quantitative detection of CTV in citrus and aphids has also been developed based on real-time RT-PCR, which can detect the pathogen even at low titer in the tissue and thus considered as gold standard technique (Saponari et al.2008; Bertolini et al. 2008). In recent time, different advanced molecular techniques are employed for early detection of CTV viz., RT-LAMP (Reverse transcription loop-mediated isothermal amplification), IC-RT-LAMP (Immunocapture-reverse transcription loop-mediated isothermal amplification), and CTV-RT-RPA-LFICA (Reverse transcription recombinase polymerase amplification lateral flow immuno-chromatographic assay) (Warghane et al. 2017a,b; Selvaraj et al. 2019; Ghosh et al. 2020a). However, there is no report of using these methods in determining CTV distribution in infected citrus plant but employing them would be an important and proper selection method for an accurate diagnosis as well as the targeted disease management.

CTV titer assessment in different tissue samples of the affected tree could be performed using quantitative real-time RT-PCR. The virus distribution in plant system is influenced by different factors, viz., tissue type, host-virus interaction, and environmental conditions (Kogovsek et al. 2011). The pathogen can be temporarily inactivated or reduced its titer due to high temperature (Roistacher et al. 1974) and when the temperature reduces, the viral titer increases. The viruses enter in plant system by different modes and move from one tissue to another tissue via the plasmodesmata and communication channels (Caldwell 1930; Agrios 1988; Leisner and Turgeon 1993; Motghare et al. 2018). The movement and distribution of CTV within infected plant is unknown yet. Therefore, the utilization of the sensitive method for early detection of CTV is needed to better management of tristeza disease. In view of this scenario, the present study was undertaken to standardize TaqMan real-time RT-PCR for CTV detection and its application to determine CTV distribution in tissues of citrus plants to select the particular tissue with the highest viral titer.

Materials and methods

Field sampling: selection of citrus trees, tissue sampling and processing

Experiment was conducted using sweet orange (*C. sinensis*) plants, orchard block number 129 at ICAR-Central Citrus Research Institute, Nagpur, India. The field-grown 10–12-year old naturally infected four sweet orange trees were selected for CTV distribution study by conventional RT-PCR and real-time RT-PCR. The selected CTV-infected citrus plants served as the primary tissue source for CTV quantification assay. Eleven different tissue samples viz., shoot tip, feeder roots, twig bark (with phloem tissue), asymptomatic leaf lamella, symptomatic leaf lamella, asymptomatic leaf midrib, symptomatic leaf midrib, fruit peel, fruit pulp, seed and partially dead twig bark were collected from four CTV-infected and two healthy sweet orange plants (Fig. 1). The collected feeder roots, twig bark, leaf samples, fruits and partially dead twigs were washed with water to remove clay particles, wiped with 70% ethanol and blotted dry. Fruit's peel, pulp and seeds were excised from the fruits and stored at − 80 °C in deep freeze.

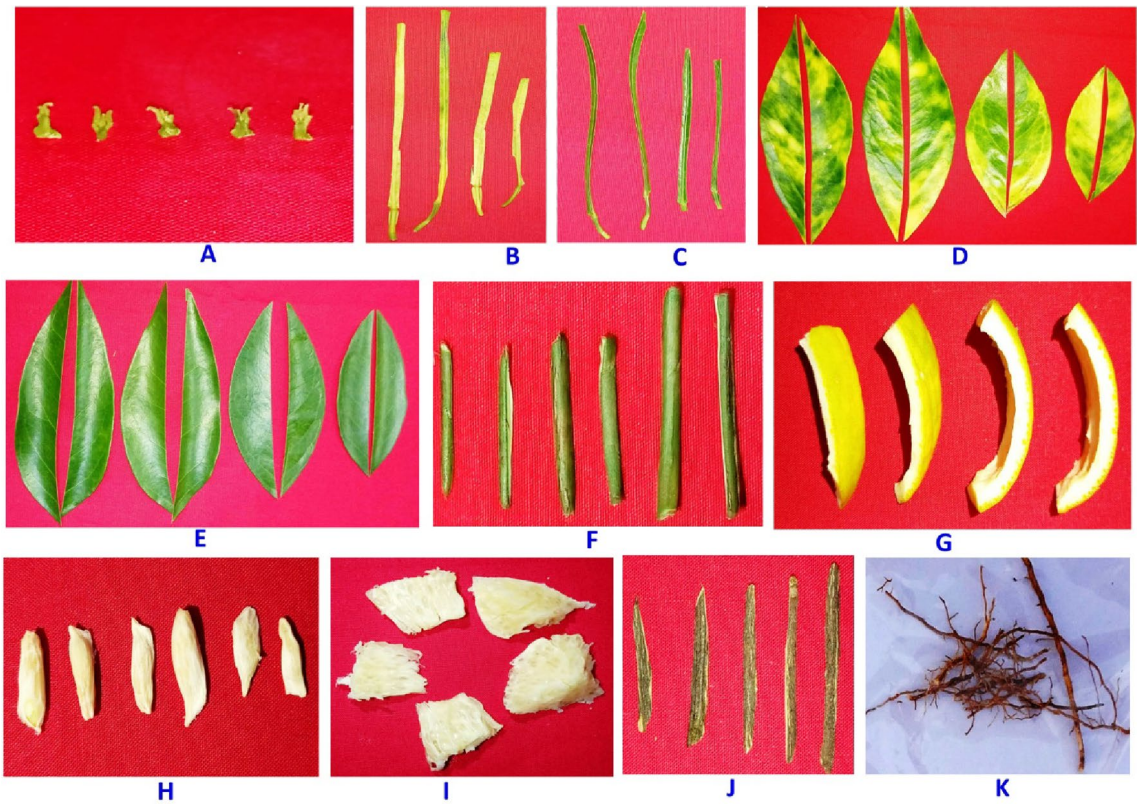

Fig. 1 Primary tissue source used for CTV distribution study. **A** Shoot tips, (**B**) Symptomatic leaf midrib, (**C**) Asymptomatic leaf midrib, (**D**) Symptomatic leaf lamella, (**E**) Asymptomatic leaf lamella, (**F**) Bark, (**G**) Fruit peel, (**H**) Seed, (**I**) Fruit pulp, (**J**) Partially dead twig bark, (**K**) Feeder roots

Primer and probe design

For TaqMan real-time RT-PCR assay, the CTV coat protein (CTV-p25) gene (GenBank AF260651)-specific primer (P25-F/R) and probe (CTV-FAM) were custom-synthesized from IDT (Coralville, USA). The probe was labeled with FAM reporter dye (6-carboxy-fluorescein) at the 5′ end, and the BHQ-1 (Black Hole Quencher) dye at the 3′ end (Table 1). The plant cytochrome oxidase gene (GenBank CX297817)-specific primers (COX-F/R) and corresponding probe (COX-P) were synthesized and used as positive internal control to assess the quality of RNA in reaction cocktails (Li et al. 2006; Ghosh et al. 2018a,b). The COX probe was labeled with JOE reporter dye at the 5′ end and the BHQ-2 at the 3′ terminal. To confirm the presence of CTV, a coat protein gene-specific primer pair (CN150/CN151) and RNA-binding-protein gene (CTV-P23)-specific primers pair (P23RBP-F/R) were used in conventional RT-PCR (Kokane et al. 2020b). The standard parameters of CTV-specific primers were taken into consideration using primer 3v.0.4.0 tool (http://bioinfo.ut.ee/primer3-0.4.0/).

Total RNA extraction, cDNA synthesis, and conventional RT-PCR

To detect CTV, leaf samples displaying tristeza symptoms were collected from field-grown sweet orange trees. The midrib tissues were excised, minced and ground using autoclaved mortar and pestle in liquid nitrogen. Total RNA was extracted from 100 mg of powdered sub-sample using RNeasy Plant Mini Kit (Qiagen, Germany). Quality of the extracted RNA was checked on 1.2% DEPC-treated agarose gel and the RNA was treated with 2U TURBO DNase (2 U/µl). Concentration of RNA was determined using NanoDrop 2000 Spectrophotometer (Thermo Scientific) and stored at − 80 ℃. The coat protein gene (CTV-p25)-specific cDNA was prepared in 15 µl reaction using 0.4 µM reverse primer (CN151), 0.5 mM dNTP, 1X first-strand buffer, 15.6 U of RNAsin (Promega), M-MuLV-RT (120 U, Promega) and 2 µg of total RNA. The reaction was performed in a T100 ™ thermal cycler (Bio-Rad, USA) at 42 °C for 50 min. The PCR amplification was carried out using synthesized cDNA as a template in a 25 µl reaction volume with 1.25U of GoTaq flexi DNA polymerase, 0.2 µM of each primer

Table 1 Primer and probe sequences used for conventional RT-PCR, generation of in vitro RNA standard and TaqMan RT-PCR assay

Sr. No	Primer/Probe code	Sequence (5′- 3′)	Length (nts)	Amplicon Size	target gene
TaqMan RT-PCR assay					
1	P25-F	AGCRGTTAAGAGTTCATCATTRC	23	~101 bp	Coat protein gene (CTV-p25)
2	P25-R	TCRGTCCAAAGTTTGTCAGA	20		
3	CTV-FAM (Probe)	56-FAM/CRCCACGGGYATAACGTA CACTCGG/3BHQ_1	25		
4	COX-F	GTATGCCACGTCGCATTCCAGA	22	~68 bp	Plant cytochrome oxidase
5	COX-R	GCCAAAACTGCTAAGGGCATTC	22		
6	COX-P (Probe)	56-JOEN/ATCCAGATGCTTACGCTG G/3BHQ_2	19		
Conventional RT-PCR					
1	CN150	ATATATTTACTCTAGATCTACCATGGA CGACGAAACAAA	39	~672 bp	Coat protein gene (CTV-p25)
2	CN151	GAATCGGAACGCGAATTCTCAACG TGTGTTAAATTTCC	38		
3	P23-RBP-F	ATGAACGATACTAGCGGAC	19	~630 bp	RNA-binding-protein gene (CTV-p23)
4	P23-RBP-R	GATGAAGTGGTGTTCACGG	19		
Generation of in vitro-transcribed RNA standard					
1	RPARNA-P25-F1	GAATTAATACGACTCACTATAGGG AGAATGGACGACGAGACGAAGAAA TTG	51	~700 bp	Coat protein gene (CTV-p25)
2	RPARNA-P25-R2	TCAACGTGTGTTAAATTTCCC	21		

The underline indicates the RNA polymerase T7 promoter sequence in the primer

(CN150/CN151), 1 × PCR buffer, 0.2 mM dNTPs mix, and 1.5 mM $MgCl_2$. The reaction was performed with the PCR program, one cycle of 2 min at 94 °C followed by 35 cycles of 30 s at 94 °C, 45 s at 61 °C, 1 min at 72 °C and final extension for 5 min at 72 °C. The presence of CTV in Mosambi plants was also confirmed by targeting an RNA-binding-protein gene, which is located towards the 3' end and adjacent to the UTR region of the CTV-RNA genome. The conventional RT-PCR was performed using the primer set P23RBP-F/R with one cycle of 2 min at 94 °C followed by 35 cycles of 30 s at 94 °C, 45 s at 52 °C, 1 min at 72 °C, and final extension at 72 °C for 5 min.

Generation of in vitro-transcribed RNA

To assess the sensitivity of the TaqMan real-time RT-PCR assay and quantify the virus titer in different tissues of Mosambi, an in vitro-transcribed RNA standard was generated from the 700 bp coat protein gene of CTV using a MEGAscript T7 transcription kit (Invitrogen) (Kokane et al 2021b). The CTV-RNA was converted into cDNA using a coat protein gene-specific reverse primer (RPARNA-P25R2). The synthesized cDNA was amplified using RPARNA-P25F1/R2 primers which contains the RNA polymerase T7 promoter site (Table 1) and amplicons were checked on 1% agarose gel, eluted and sequenced. The CTV-specific PCR product of coat protein gene was validated by sequencing and used as template (120 ng) for *in-vitro* transcription. The transcription reaction consisting 3 mM of each T7 NTPs, 2 µl enzyme mix, 1X T7 reaction buffer was performed at 37 °C for 4 h. The successfully transcribed RNA was treated with 2U TURBO DNase (2U/µl) and precipitated using lithium chloride. The recovered RNA was quantified and stored at − 80 °C.

TaqMan real-time RT-PCR assay

To determine the virus load in different tissue samples of Mosambi plant, a CTV-specific TaqMan real-time RT-PCR assay was optimized using coat protein gene-specific primers (P25-F /R) and corresponding probe (CTV-P) with an expected amplicons length of 101 bp. A primer–probe combination (COX-F/R-COX-P) targeting a 68 bp amplicons of the plant cytochrome oxidase, a housekeeping gene were used to normalize the cycle threshold (Ct) values. Total CTV-RNA was converted into cDNA using a targeted gene-specific reverse primer (P25-R) and cytochrome oxidase gene-specific reveres primer (COX-R). Total 50 ng of cDNA was used as a template in TaqMan real-time RT-PCR reactions. Before starting the reaction, the 17 µl of CXR reference dye was mixed in 1 ml of GoTaq probe qPCR master mixture (promega). The optimum reporter fluorescence and the lowest Ct value were achieved by optimizing the concentrations of

all possible combinations 50, 100, 150, 200, 250, 300, and 350 nM for each primers and probe. The assay was performed using a StepOne Real-Time PCR System (Applied Biosystems) in a total of 20 µl reaction volume containing the reagents at optimized concentrations: 300 nM P25-F/R target primers, 250 nM target probe (CTV-FAM), 300 nM (each) internal control primers (COX-F and COX-R), 250 nM internal control probe (COX-P) with GoTaq q PCR master mix and 50 ng of cDNA. The reaction protocol of 95 °C for 2 min, followed by 40 cycles at 95 °C for 15 s, and 60 °C for 1 min was used. All experimental reactions were performed in triplicate along with non-template controls and StepOne Software v2.1 used for data analysis. Sensitivity of the optimized assay was assessed using in vitro-transcribed RNA as template. Standard curve and amplification efficiency was determined using tenfold serial dilution of 5.95 ng/µl RNA (1, 10^{-1}, 10^{-2}, 10^{-3}, 10^{-4}, 10^{-5}, 10^{-6}, 10^{-7}, 10^{-8}, and 10^{-9}).

Quantitative distribution of CTV and data analysis

CTV load in different tissues of sweet orange tree was determined by real-time RT-PCR. Eleven different tissue samples viz., shoot tip, feeder roots, twig bark, asymptomatic leaf lamella, symptomatic leaf lamella, asymptomatic leaf midrib, symptomatic leaf midrib, fruit peel, fruit pulp, seed and partially dead twig bark of experimental plants were checked to analyze the CTV load using real-time RT-PCR with TaqMan chemistry. The CTV genome copy numbers in tissue samples were determined using the standard curve method generated with known concentration of in vitro-transcribed RNA as template. The RNA copy number was determined using the formula, copy number = Moles of ssRNA x Avogadro's number (6.022×10^{23}). The moles of ssRNA were calculated as mass of ssRNA (g)/ [(number of ribonucleotides of ssRNA × average molecular weight of a ribonucleotide) + 18.02 g/mol]. The 59.57 ng/µl of RNA was tenfold serially diluted and standard curve was generated with the obtained Ct values by StepOne Software v2.1. The standard linear regression equation was obtained. Finally, CTV genome copy numbers in each tissue samples were calculated by extrapolating the average Ct values of the samples into the standard curve. The three technical replicates were used to run the TaqMan real-time RT-PCR for each tissue sample and the mean Ct value was used to calculate viral copy number. The equal quantity of sample and RNA template was used to determine the CTV genome copy number. Additionally, a housekeeping COX gene was used as internal control for normalization of the target gene, which was amplified in parallel with target gene.

Results

Selection of experimental plants by conventional RT-PCR

Fifty-five field-grown Mosambi plants were screened for CTV using RT-PCR, and fifteen plants found positive for CTV. Among these, four plants having approximately similar pathogen load and showed more intense CTV-specific ~ 672 bp band on agarose gel (Fig. 2A) were further used for virus distribution study. Further, all tissue samples used in the present study ($n = 11$) were also tested by conventional RT-PCR and a ~ 672 bp amplicon was successfully amplified from six out of the eleven tissues. The shoot tip, fruit cover/peel, fruit seed, fruit pulp and partially dead twig bark did not show any amplification (Fig. 2A). The presence of CTV in selected experimental Mosambi plants and all tissue samples also confirmed with conventional RT-PCR using RNA-binding gene-specific primers and same result was observed (Fig. 2B) (Fig. 3).

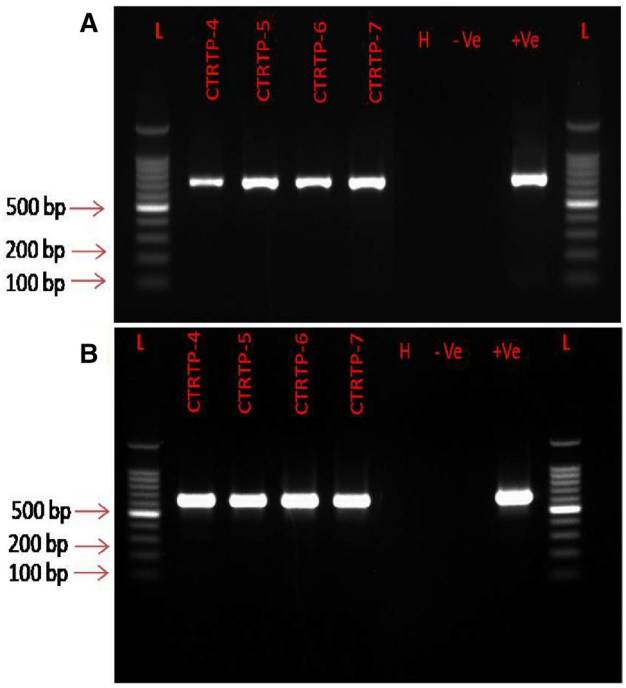

Fig. 2 An agarose gel electrophoresis photograph of amplicons obtained from CTV-infected citrus plants samples by a conventional RT-PCR. **A** Coat protein (CTV-p25) gene amplicons using the primer set CN150/CN151. **B** CTV-p23 gene amplicons using the primer set p23-RBP-F/-R. Lane, L-100 bp marker, Lane-1: CTRTP-4 plant, Lane-2: CTRTP-5 plant, Lane-3: CTRTP-6 plant, Lane-4: CTRTP-7 plant, Lane-5: Healthy plant, Lane-6: Negative control and Lane-7: Positive control

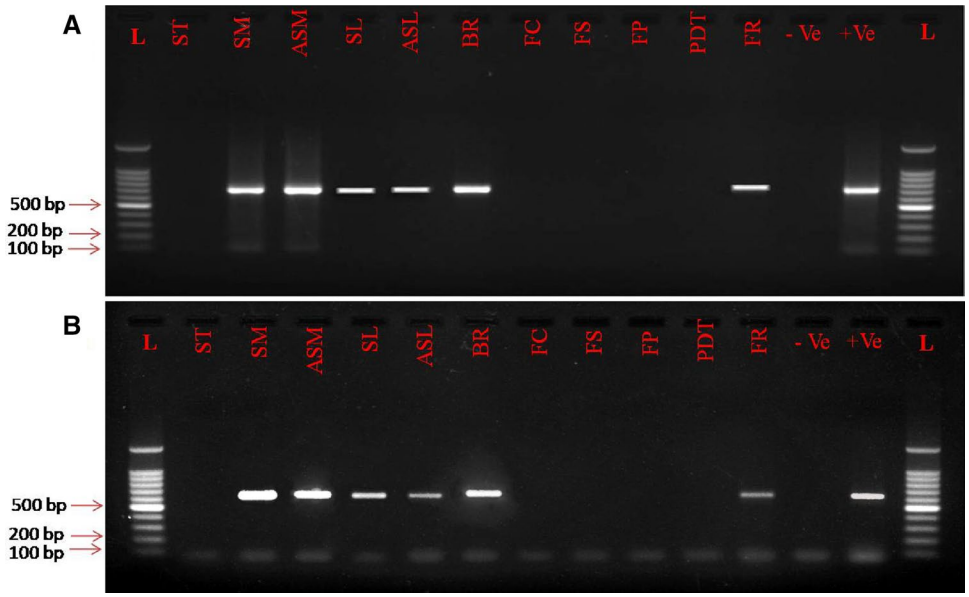

Fig. 3 An agarose gel electrophoresis photograph of CTV-specific amplicons obtained from eleven citrus tissues by a conventional RT-PCR. **A** Coat protein (CTV-p25) gene amplicons using the primer set CN150/CN151. **B** CTV-p23 gene amplicons using the primer set p23-RBP-F/-R. Lane, L-100 bp marker, Lane-1: *ST* Shoot tips, Lane-2: *SM* Symptomatic leaf midrib, Lane-3: *ASM* Asymptomatic leaf midrib, Lane-4: *SL* Symptomatic leaf lamella, Lane-5: *ASL* Asymptomatic leaf lamella, Lane-6: *BR* Bark, Lane-7: *FC* Fruit peel/cover, Lane-8: *FS* Fruit seed, Lane-9: *FP* Fruit pulp, Lane-10: *PDT* Partially dead twig bark, Lane-11: *FR* Feeder roots, Lane-12: Negative control and Lane-13: Positive control

Efficiency and sensitivity of CTV-TaqMan real-time RT-PCR

The TaqMan RT-PCR for CTV was standardized using coat protein gene-specific primer–probe combinations (P25-F/R-CTV-FAM). The assay consistently detected in vitro-transcribed pure CTV-RNA at concentrations ranging from 0.0595 fg to 5.95×10^6 fg (Fig. 4A). The standard curve was generated with observed exponential amplification and standard fluorescence. The exponential relationship

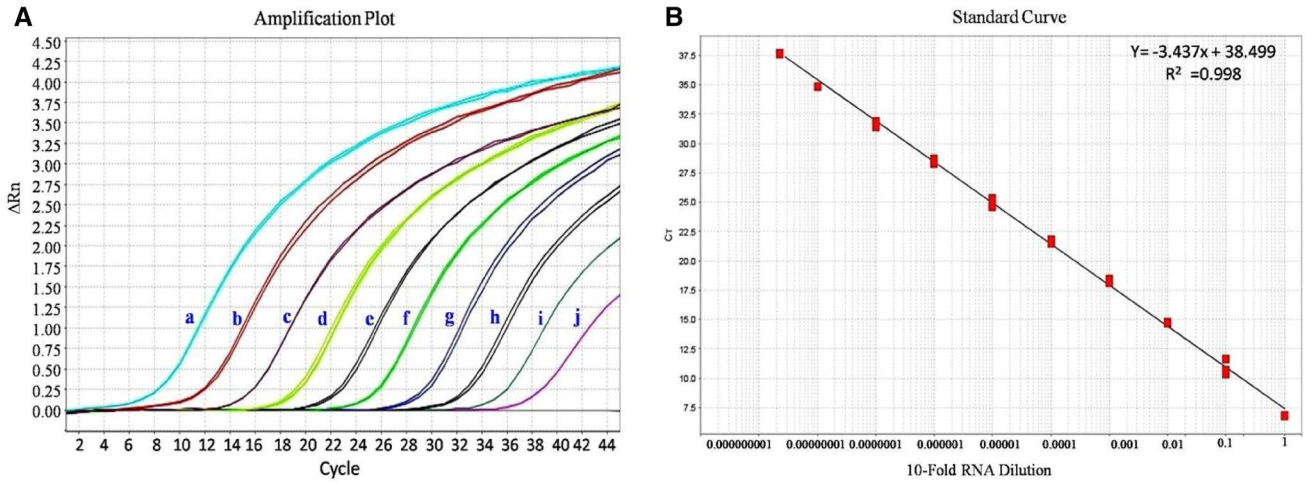

Fig. 4 Sensitivity analysis of CTV-TaqMan reverse transcription-PCR assay. **A** Amplification plot generated using tenfold serial dilution of known concentration of in vitro-transcribed RNA of CTV. The 5.95 ng of RNA was serially diluted as, Line-a = 1, Line-b = 10^{-1}, Line-c = 10^{-2}, Line-d = 10^{-3}, Line-e = 10^{-4}, Line-f = 10^{-5}, Line-g = 10^{-6}, Line-h = 10^{-7}, Line-i = 10^{-8}, and Line-j = 10^{-9}. **B** The standard curve established between RNA concentrations vs. cycle threshold (Ct) obtained using tenfold serial dilution of 5.95 ng of in vitro-transcribed RNA of CTV. A Ct value of 6.84 was obtained for the 5.95 ng (Line-a) in vitro RNA transcripts. Whereas very low fluorescence was observed for 10^{-9} dilutions (Line-j)

between the concentration of in vitro-transcribed CTV-RNA and Ct value was robust with a regression coefficient (R^2) of 0.999 (Fig. 4B). The obtained regression coefficient values suggest that the standardized assay was very sensitive and efficient, with the pathogen detection limit of > 0.0595 fg of in vitro-transcribed RNA (Ct value = 34.53). However, the detection limit of the standardized assay was reduced 10 times when the template (in vitro-transcribed pure CTV-RNA) pulled with healthy citrus total RNA. The standardized assay for the concentration of primer–probe combinations was able to detect the CTV at very low titer in Mosambi plant tissue samples. Therefore, CTV-TaqMan real-time RT-PCR assay was used subsequently for virus distribution study.

The absolute CTV titer quantification

To determine the absolute CTV genome copy number in citrus plant tissue samples, the standard curve showing an exponential amplification of target gene by at least 3.34 orders of magnitude with $R^2 = 0.998$ and Eff% = 95.41 was used. The in vitro-transcribed RNA as an initial template with copy number of 1.062×10^9 showed an average Ct value of 6.84. The quantification of CTV copy number in different tissue samples of Mosambi plants was accomplished based on standard curve regression equation $Y = -3.437 \times +38.499$ (Fig. 5). The tissue samples having average Ct value > 36 were considered negative for CTV.

CTV distribution in field-grown Mosambi plants

Four field-grown Mosambi plants were screened for CTV distribution for two consecutive months and the virus copy number was estimated in each sample collected during this period. Eleven tissue samples were assessed for pathogen load and observed that titer of CTV varied in different tissue. The CTV titer in particular tissue was also influenced by temperature. In the start of summer season, in the month of March (2018) (Highest temp = 41 ℃, Average temp = 29 ℃, Lowest temp = 17 ℃), the viral load was highest in midrib tissue of the symptomatic leaf (virus loads ranging from 4.1×10^7–1.4×10^8/100 mg of tissue), followed by other tissues like midrib tissue of the asymptomatic leaf (2.2×10^7–6.7×10^7/100 mg), symptomatic leaf lamella (1×10^7–2.3×10^7/100 mg), asymptomatic leaf lamella (1.6×10^7–2×10^7 /100 mg), twig bark (2.3×10^7–3.8×10^7 /100 mg), feeder roots (8.8×10^6–1.9×10^7 /100 mg) and the lowest virus titer was detected in fruit cover (3.8×10^5–9.8×10^5/100 mg), fruit seed (9.2×10^4–2×10^5/100 mg), fruit pulp (2.6×10^4–9.8×10^4/100 mg), partial dead twigs (1×10^3–1.7×10^4/100 mg) and shoot tip (2.3×10^3–4.5×10^3/100 mg) (Fig. 6A). However, in the hottest month of summer season, May (2018) (Highest temp = 45 ℃, Average temp = 37 ℃, Lowest temp = 24 ℃), the highest CTV load was observed in the feeder roots (3×10^7 to 1.1×10^8 /100 mg) than midrib tissues of symptomatic leaf (1.7×10^6–1.6×10^7/100 mg) followed by other tissues like midrib tissue of the asymptomatic leaf (2.3×10^6 to 6.3×10^6/100 mg), symptomatic leaf lamella (1.6×10^6–9.8×10^6/100 mg), asymptomatic leaf lamella (7.6×10^5–8.9×10^6/100 mg), twig bark (4.0×10^6 to 1.3×10^7/100 mg), and the lowest virus titer was found in fruit cover (2.5×10^5–8.4×10^5/100 mg), fruit seed (9.8×10^4–1.9×10^5/100 mg), fruit pulp (9.9×10^3–6.2×10^4/100 mg), shoot tip

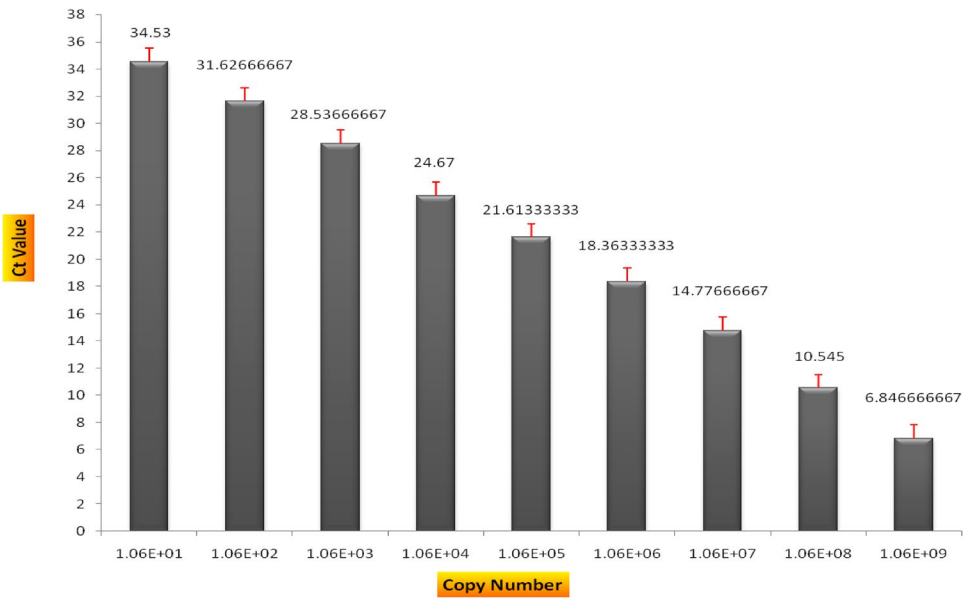

Fig. 5 The quantification of CTV genome copy number by extrapolating with the standard curve. The graph represents the exponential relationship between CTV genome copy number and Ct (Cycle Threshold) value. The Y-axis represents Ct value and X-axis represents virus copy number

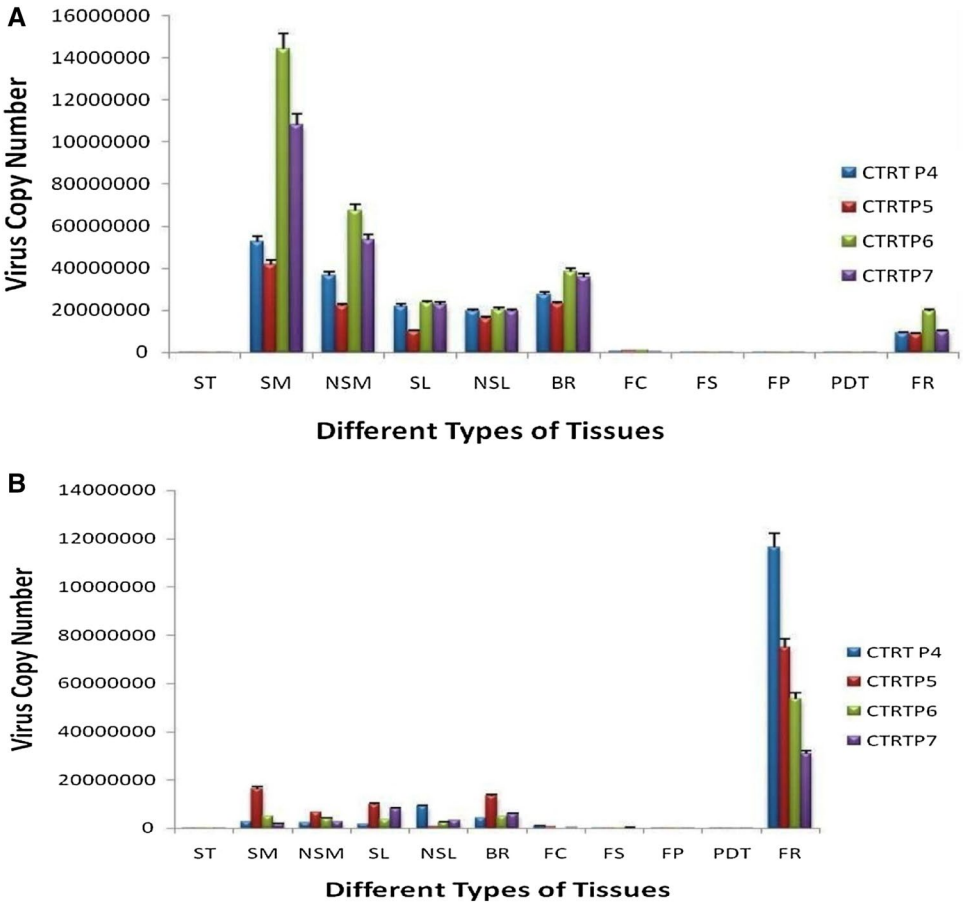

Fig. 6 Distributions of CTV load in different plant tissues as measured by a TaqMan RT-PCR (**A**), In the month of low temperature (Low temp = 17 °C, High temp = 41 °C, Average temp = 29 °C). (**B**) In the month of high temperature (Low temp = 24 °C, High temp = 45 °C, Average temp = 27 °C). The Y-axis represents virus copy number/ 100 mg of tissue, and four different bars represent four different experimental plants; X-axis represents different tested tissues, *ST* Shoot tip, *SM* Symptomatic leaf midrib, *NSM* Non-symptomatic leaf midrib, *SL* Symptomatic leaf lamella, *NSL* Non-symptomatic leaf lamella, *BR* Twig bark, *FC* Fruit cover, *FS* Fruit seed, *FP* Fruit pulp, *PDT* Partially dead twig, *FR* feeder roots

(1.1×10^3–8.7×10^3/100 mg) and partial dead twigs ((9.1×10^2–3.2×10^3/100 mg) (Fig. 6B). All eleven tissue samples were grouped into three categories based on viral load: high (median value: 1×10^7), moderate (median value: 4.2×10^4), and low (median value: 4.2×10^4). The tissues grouped under high-load categories are symptomatic leaf midrib**,** asymptomatic leaf midrib, feeder roots, twig bark, symptomatic leaf lamella, and asymptomatic leaf lamella, whereas the fruit cover, fruit seed tissue grouped under moderate-load categories. Partially dead twig and shoot tip tissue showed very low titer, thus grouped under low-titer categories. To generate comprehensive data on virus distribution in the diseased tree, the average CTV load in different tissues for each tree was plotted into a box-whisker graph (Fig. 7).

Discussion

Tristeza disease caused by CTV has ranked as one of the most economically important citrus diseases that changed the course of the citrus industry (Moreno et al. 2008). The CTV epidemics have considerably affected the productivity and destroyed over 100 million of fruit-bearing citrus trees in the last several decades worldwide (Dawson et al. 2013). The infection process, tropism, and distribution of the CTV in the citrus plant system are not known well and hence there is a lack of understanding of how the virus causes decline in some citrus cultivars but not in others (Harper et al. 2014). CTV is adapted to replicate in the phloem cells, however, it moves throughout the phloem system of citrus plants unevenly (Fu et al. 2017). It is speculated that CTV exhibits a phloem-limited tropism in citrus plants mainly by long-distance movement and very less by cell-to-cell movement in phloem-associated cells (Harper et al. 2014). Therefore, long-distance movement mechanisms are considered as target pathway for obtaining host resistance and preventing a systemic spread of the virus. The virus moves through sieve elements from one tissue to another in the plant system and intermittently enters an adjacent companion or phloem parenchyma cell. The proportion of cell-to-cell movement of the CTV from phloem to an adjacent companion/parenchyma cell varied in different plant species, which may be because of variation in the susceptible and permissive nature of host cells to facilitate viral entry. This indicates that the host resistance plays a considerable in CTV infection and viral tropism in the citrus. It is also speculated that the tolerant citrus host reduces the movement efficacy of CTV in both long-distance and cell-to-cell movement (Dawson et al.

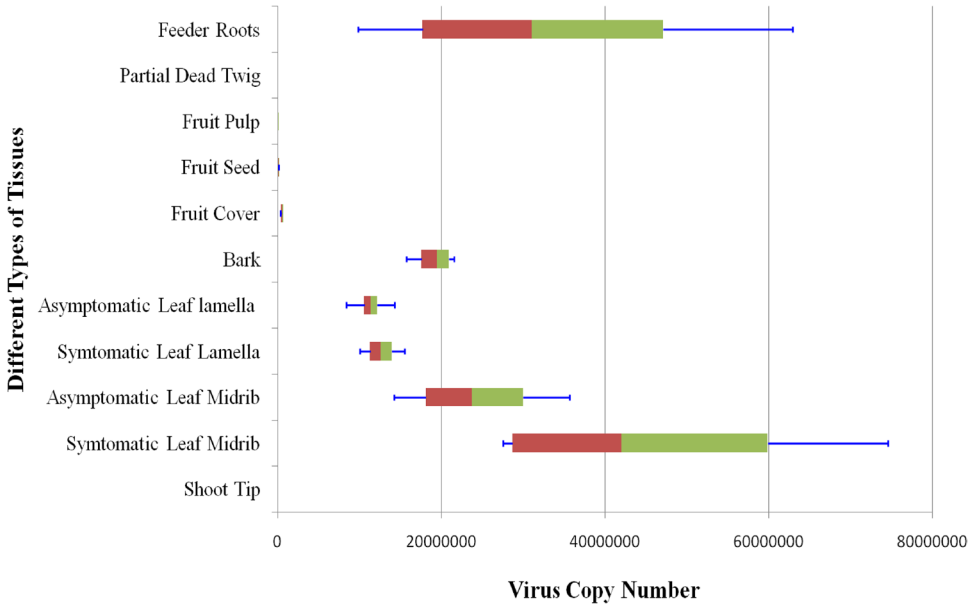

Fig.7 Box and whisker plot analyses of virus copy number in CTV-infected plants. The graph represents the sample distribution, right side whisker shows upper extreme value, left side whisker shows lower extreme value among the tested samples and the interquartile range is represented by width of the box. In each box, the middle line represents a median value of the viral load

2013; Harper et al. 2014). There are different genes of the virus, which are reported to be involved in the host–virus interactions to extend its host range (Tatineni et al. 2011). The dynamics of viral population and distribution dictate the pathogenicity of the infection. Moreover, there is little understanding of the factors that influence CTV titer dynamics. Understanding the correlation among the virus population dynamics, factors affecting virus population dynamics, tropism, distribution, and pathogenicity are attributed to early disease diagnosis and management. Therefore, an implementation of the reliable molecular diagnostic technique in virus distribution study is an essential tool to understand how the virus moves and in which tissue it gets accumulated with maximum concentration. Determining virus distribution in a citrus plant will help in early disease diagnosis by selecting appropriate tissue containing high CTV titer. This would enable to avoid disease spread and economic losses due to the disease in the citrus industry. Tarafdar et al. (2012) studied *in planta* distribution, accumulation and movement of CTV in citrus host using ELISA and conventional RT-PCR. They observed an uneven distribution of CTV in all the plant parts including high titer in the tender bark, petiole and mid-rib tissue. However, the CTV distribution study was analyzed semi-quantitatively by ELISA and conventional RT-PCR in different tissue and lacked absolute virus titer data.

We described here a TaqMan real-time RT-PCR assay to determine virus distribution and titer precisely in a diseased tree. The TaqMan RT-PCR was optimized using CTV coat protein gene-specific primer–probe combinations (P25-F/R-CTV-FAM). The assay was very sensitive and efficient, detected in vitro-transcribed CTV-RNA at concentration > 0.0595 fg. The in vitro-transcribed RNA template pulled with healthy citrus total RNA in the reaction showed effect on the assay by reducing the tenfold detection limit. However, the assay was able to detect the CTV efficiently at very low titer in tissue samples. The standardized TaqMan real-time RT-PCR assay was further implemented for virus distribution study in eleven different tissues of sweet orange. The virus distribution study observed a highest CTV titer in the midrib tissue of the symptomatic leaf followed by other tissues like midrib tissue of the asymptomatic leaf, symptomatic leaf lamella, asymptomatic leaf lamella, twig bark, feeder roots and lowest virus titer were found in fruit cover, fruit seed, fruit pulp, partial dead twigs and shoot tip. The high CTV load was recorded in the midrib tissue of symptomatic and asymptomatic leaf than their lamella tissue, suggesting that the virus resides and moves through the phloem from one region to another, moreover also crosses the boundary. Thus, it suggests that the tropism of CTV is not only restricted to phloem but also has access towards other tissues or organs (Harper et al. 2014). The result signifies that symptom expression is directly proportional to the virus load. It is also observed that when temperature rises in summer, CTV titer in the different tissues decreases as compared to normal temperature. It was interesting to note that the highest CTV titer was recorded in the root system during hot summer. The fluctuation in the virus titer in the different tissues may be because of either inhibition of virus replication or virus movement in the phloem from one tissue to another at high temperature. Temperature fluctuations within infected plants are also considered to influence the viruses by disrupting the balance between viral replication and degradation. The higher temperature than the optimum impedes the virus replication and causes its deterioration (Cowell et al. 2016). The higher CTV titer in the root system

during high environmental temperatures suggests that temperature may have less influence on viral replication in the underground roots than it does in other sunlight-exposed tissues. The higher titer of virus in the root system may act like reservoir and may be involved in re-infection towards the citrus canopy during cold condition. The high CTV titer was also observed in the twig bark which was active in the sap transport from one tissue to other.

There are numbers of reports which have demonstrated that most of the viruses cannot be transported by seed. However, some viruses/pathogen which are seed-borne can be transferred in the next generation of the plants (vertical transmission). More than 232 plant virus and viroid diseases are reported to be seed-transmissible by different methods like entrance to the seedling after germination via infected seed coat, virus invasion of the embryo from infected tissues or through infected pollen grains (Fabre et al. 2014; Kil et al. 2016). The transmission of CTV also takes place through budding/grafting and different aphid vectors, but seed transmission of CTV has not reported previously. Interestingly, CTV-specific amplification was not observed in the shoot tips, fruit cover, fruit seeds, fruit pulp and partially dead twigs of CTV-infected citrus plant by conventional PCR but found positive with real-time PCR. Although the fruit tissues observed positive with TaqMan real-time RT-PCR, *i.e.,* fruit peel, fruit pulp and fruit seeds, the titer of CTV was very low. This is the first report of presence of CTV in the fruit tissues of infected citrus plant. As we have tested entire mosambi seed, there is need to study all the tissues of fruit seed separately to confirm the actual location of CTV in the seed. Very low CTV titer was recorded in the twig bark (partially dead) which was in the vicinity of the dead twig that confirmed that virus moves systematically through the phloem to spread to uninfected areas. Absence or very low titer of the virus in the partially dead twig bark tissue could be attributed towards the dry phloem or very little flow of sap (Tarafdar et al. 2012). Although the partially dead twigs carry very low virus copy, they may act as virus carrier and facilitate disease spread to healthy plants during pruning via mechanical means. Meristem tissue culture is a widely used approach for virus eradication from various commercial horticultural crops by anticipating it would be virus-free. In the present study, low CTV titer was observed in the shoot tip that may be because of inability of virus to reach in the fast growing meristematic tissue or undeveloped vascular system (Motghare et al. 2018). Our study suggests that there is a need to be more careful while production of virus-free planting materials using shoot tip explants. It would be best to use as possible as small shoot tip explants to avoid the entry of the CTV and for the production of virus-free planting material. Combined use of meristem culture, thermotherapy and cryotherapy is also emerging approach for production of virus-free planting material (Vivek et al. 2018).

The highest virus titer was observed only in the tissue that contains the phloem system, *i.e.,* mid-rib tissue, root system, tender twig bark and other tissue, indicating that mostly virus moves from infected tissue to healthy tissue via phloem system. However, a low titer of virus also recorded in the fruit tissues that indicated accumulation of the virus in the non-phloem containing tissue by short-distance cell-to-cell movement. Overall, the study clearly demonstrates that CTV is primarily located in the phloem, companion cells and systematically circulated throughout the plant system. The virus was occasionally found in the mesophyll, epidermis and fruit tissues (Bar-Joseph et al. 1979; Garnsey et al. 1998). Thus, the study will be helpful in selecting an appropriate tissue sample for virus indexing of mother plants in Budwood Certification Programme.

Acknowledgements This research was funded by the project ICAR-CRP on Vaccines and Diagnostics, Govt. of India F. No.16-11/PP/ICAR-CRP/17-18/06. Authors thank Dr. Arun Kumar Dhar, University of Arizona, Tucson, Arizona 8572, USA for reviewing this manuscript. The authors declare there are no competing interests.

Author contributions Conceptualization: DKG, SBK, AJW, PM; Methodology: SBK, AJW, ADK, DS, MGG; Formal analysis and investigation: DKG, SBK, AJW; Writing—original draft preparation: SBK; Writing—review and editing: DKG, SBK; Funding acquisition: DKG, MKR; Resources: DKG; Supervision: DKG, PM, MKR. All authors read and approved the final manuscript.

Funding This research was funded by ICAR- Consortia Research Platform (CRP) on Vaccines and Diagnostics, ICAR, Government of India, New Delhi. F.No.16–11/PP/ICAR-CRP/17–18/06.

Data availability The data that support the findings of this study are available from the corresponding author upon reasonable request.

Declarations

Consent for publication I, the undersigned, give my consent for the publication of identifiable details, which can include photograph(s) and details within the text ("Material") to be published in the 3 Biotech. Therefore, anyone can read material published in the Journal.

References

Agrios GN (1988) Plant diseases caused by viruses. Plant Pathol, 3rd edn. Academic Press, pp 622–722

Ahlawat YS (1997) Viruses, greening bacterium and viroids associated with citrus (*Citrus* spp.) decline in India. Indian J Agric Sci 67:51–57

Albiach-marti MR, Robertson C, Gowda S, Tatineni S, Belliure B, Garnsey SM et al (2010) The pathogenicity determinant of *Citrus tristeza virus* causing the seedling yellows syndrome maps at the 3′-terminal region of the viral genome. Mol Plant Pathol 11:55–67. https://doi.org/10.1111/j.1364-3703.2009.00572.x

Bar-Joseph M, Garnsey SM, Gonsavales D (1979) The Closteroviruses: a distinct group of elongated plant viruses. Adv Virus Res 25:93–168. https://doi.org/10.1016/S0065-3527(08)60569-2

Bar-Joseph M, Marcus R, Lee RF (1989) The continuous challenge of *Citrus tristeza virus* control. Ann Rev Phytopathol 27:291–316. https://doi.org/10.1146/annurev.py.27.090189.001451

Bertolini E, Moreno A, Capote N, Olmos A, de Luis A, Vidal E et al (2008) Quantitative detection of *Citrus tristeza virus* in plant tissues and single aphids by real-time RT-PCR. Eur J Plant Pathol 120:177–188. https://doi.org/10.1007/s10658-007-9206-9

Biswas K, Tarafdar A, Sharma S, Singh J, Dwivedi S, Biswas K et al (2014) Current status of *Citrus tristeza virus* incidence and its spatial distribution in citrus growing geographical zones of India. Indian J Agric Sci 84:184–189

Caldwell J (1930) The physiology of virus diseases in plants: the movement of mosaic in the tomato plant. Ann Appl Biol 17:429–443. https://doi.org/10.1111/j.1744-7348.1930.tb07224.x

Cowell SJ, Harper SJ, Dawson WO (2016) Some like it hot: *Citrus tristeza virus* strains react differently to elevated temperature. Arch Virol 161:3567–3570. https://doi.org/10.1007/s00705-016-3083-5

Dawson WO, Garnsey SM, Tatineni S, Folimonova SY, Harper SJ, Gowda S (2013) *Citrus tristeza* virus-host interactions. Front Microbiol 4:88. https://doi.org/10.3389/fmicb.2013.00088

Fabre F, Moury B, Johansen EI, Simon V, Jacquemond M, Senoussi R (2014) Narrow bottlenecks affect *Pea seedborne mosaic virus* populations during vertical seed transmission but not during leaf colonization. PLoS Pathog 10:e1003833. https://doi.org/10.1371/journal.ppat.1003833

Fu S, Shao J, Paul C, Zhou C, Hartung JS (2017) Transcriptional analysis of sweet orange trees co-infected with '*Candidatus* Liberibacter asiaticus' and mild or severe strains of *Citrus tristeza virus*. BMC Genom 18:837. https://doi.org/10.1186/s12864-017-4174-8

Garnsey SM, Gottwald TR, Yokomi RK (1998) Control strategies for *Citrus tristeza virus*. In: Hadidi A, Khetrapal R, Koganezawa H (eds) Plant virus disease control: principles and practices. APS Press, pp 639–658

Ghosh DK, Bhose S, Motghare M, Warghane A, Mukherjee K, Ghosh DK et al (2015) Genetic diversity of the Indian populations of '*Candidatus* Liberibacter asiaticus' based on the tandem repeat variability in a genomic locus. Phytopathol 105:1043–1049. https://doi.org/10.1094/PHYTO-09-14-0253-R

Ghosh DK, Kokane SB, Kokane AD, Warghane AJ, Motghare MR, Bhose S et al (2018a) Development of a recombinase polymerase based isothermal amplification combined with lateral flow assay (HLB-RPA-LFA) for rapid detection of '*Candidatus* Liberibacter asiaticus'. PLoS ONE 13:e0208530. https://doi.org/10.1371/journal.pone.0208530

Ghosh DK, Kokane S, Kumar P, Ozcan A, Warghane A, Motghare M et al (2018b) Antimicrobial nano-zinc oxide-2S albumin protein formulation significantly inhibits growth of '*Candidatus* Liberibacter asiaticus' in planta. PLoS ONE 13:e0204702. https://doi.org/10.1371/journal.pone.0204702

Ghosh DK, Motghare M, Kokane A, Kokane S, Warghane A, Bhose S et al (2019) First report of a '*Candidatus* Phytoplasma cynodontis'-related strain (group 16SrXIV) associated with Huanglongbing disease on *Citrus grandis*. Austr Plant Dis Notes 14:9. https://doi.org/10.1007/s13314-019-0340-y

Ghosh D, Kokane S, Gowda S (2020a) Development of a reverse transcription recombinase polymerase based isothermal amplification coupled with lateral flow immunochromatographic assay (CTV-RT-RPA-LFICA) for rapid detection of *Citrus tristeza virus*. Sci Rep 10:20593. https://doi.org/10.1038/s41598-020-77692-w

Ghosh DK, Kokane AD, Kokane SB, Tenzin J, Gubyad MG, Wangdi P et al (2020b) Detection and molecular characterization of '*Candidatus* Liberibacter asiaticus' and *Citrus tristeza virus* associated with citrus decline in Bhutan. Phytopathol. https://doi.org/10.1094/PHYTO-07-20-0266-R

Harper SJ, Cowell SJ, Robertson CJ, Dawson WO (2014) Differential tropism in roots and shoots infected by *Citrus tristeza virus*. Virology 460:91–99. https://doi.org/10.1016/j.virol.2014.04.035

Karasev AV, Boyko VP, Gowda S, Nikolaeva OV, Hilf ME, Koonin EV et al (1995) Complete sequence of the *Citrus tristeza virus* RNA genome. Virology 208:511–520. https://doi.org/10.1006/viro.1995.1182

Kil EJ, Kim S, Lee YJ, Byun HS, Park J, Seo H et al (2016) *Tomato yellow leaf curl virus* (TYLCV-IL): a seed-transmissible geminivirus in tomatoes. Sci Rep 6:19013. https://doi.org/10.1038/srep19013

Kogovsek P, Kladnik A, Mlakar J, Znidaric MT, Dermastia M, Ravnikar M et al (2011) Distribution of *Potato virus Y* in potato plant organs, tissues, and cells. Phytopathol 101:1292–1300. https://doi.org/10.1094/PHYTO-01-11-0020

Kokane SB, Bhose S, Kokane A, Gubyad M, Ghosh DK (2020a) Molecular detection, identification, and sequence analysis of '*Candidatus* Liberibacter asiaticus' associated with Huanglongbing disease of citrus in North India. 3 Biotech 10:341. https://doi.org/10.1007/s13205-020-02334-x

Kokane SB, Kokane AD, Misra P, Warghane AJ, Kumar P, Gubyad MG et al (2020b) *In-silico* characterization and RNA-binding protein based polyclonal antibodies production for detection of *Citrus tristeza virus*. Mol Cell Probes 54:101654. https://doi.org/10.1016/j.mcp.2020.101654

Kokane A, Lawrence K, Surwase D, Misra P, Warghane A, Ghosh DK (2020c) Development of reverse transcription duplex PCR (RT-d-PCR) for simultaneous detection of the *Citrus tristeza virus* and *Indian citrus ringspot virus*. Int J Innov Hortic 9(2):131–138. https://doi.org/10.5958/2582-2527.2020.00016.0

Kokane AD, Kokane SB, Warghane AJ, Gubyad MG, Sharma AK, Reddy KM et al (2021a) A rapid and sensitive reverse transcription-loop-mediated isothermal amplification (RT-LAMP) assay for the detection of Indian citrus ringspot virus. Plant Dis. https://doi.org/10.1094/PDIS-06-20-1349-RE

Kokane AD, Lawrence K, Kokane SB, Gubyad MG, Misra P, Reddy MK et al (2021b) Development of a SYBR Green-based RT-qPCR assay for the detection of *Indian citrus ringspot virus*. 3 Biotech 11:359. https://doi.org/10.1007/s13205-021-02903-8

Leisner SM, Turgeon R (1993) Movement of virus and photoassimilate in the phloem: a comparative analysis. BioEssays 15:741–748. https://doi.org/10.1002/bies.950151107

Li W, Hartung JS, Levy L (2006) Quantitative real-time PCR for detection and identification of *Candidatus* Liberibacter species associated with citrus huanglongbing. J Microbiol Methods 66:104–115. https://doi.org/10.1016/j.mimet.2005.10.018

Marroquin C, Olmos A, Gorris MT, Bertolini E, Martınez MC, Carbonell EA et al (2004) Estimation of the number of aphids carrying *Citrus tristeza virus* that visit adult citrus trees. Virus Res 100:101–108. https://doi.org/10.1016/j.virusres.2003.12.018

Moreno P, Ambrós S, Albiach-Martí MR, Guerri J, Peña L (2008) *Citrus tristeza virus*: a pathogen that changed the course of the citrus industry. Mol Plant Pathol 9:251–268. https://doi.org/10.1111/j.1364-3703.2007.00455.x

Motghare M, Dhar AK, Kokane A, Warghane A, Kokane S, Sharma AK et al (2018) Quantitative distribution of *Citrus yellow mosaic badnavirus* in sweet orange (*Citrus sinensis*) and its implication in developing disease diagnostics. J Virol Methods 259:25–31. https://doi.org/10.1016/j.jviromet.2018.05.015

Roistacher CN, Blue RL, Nauer EM, Calavan EC (1974) Suppression of tristeza virus symptoms in Mexican lime seedlings grown at warm temperatures. Plant Dis Rep 58:757–760

Saponari M, Keremane M, Yokomi RK (2008) Quantitative detection of *Citrus tristeza virus* in citrus and aphids by real-time reverse transcription-PCR (TaqMan®). J Virol Methods 147:43–53. https://doi.org/10.1016/j.jviromet.2007.07.026

Selvaraj V, Maheshwari Y, Hajeri S, Yokomi R (2019) A rapid detection tool for VT isolates of *Citrus tristeza virus* by immunocapture-reverse transcriptase loop- mediated isothermal amplification assay. PLoS ONE 14:e0222170. https://doi.org/10.1371/journal.pone.0222170

Tarafdar A, Ghosh B (2012) *In planta* distribution, accumulation, movement and persistence of *Citrus tristeza virus* in citrus host. Indian Phytopathol 65:184–188

Tatineni S, Robertson CJ, Garnsey SM, Dawson WO (2011) A plant virus evolved by acquiring multiple nonconserved genes to extend its host range. Proc Natl Acad Sci 108:17366–17371. https://doi.org/10.1073/pnas.1113227108

Vasudeva RS, Varma PM, Capoor SP, Rao DG (1959) Transmission of citrus decline virus by *Toxoptera Citricidus* Kirk in India. Curr Sci 28:418–419

Vivek M, Modgil M (2018) Elimination of viruses through thermotherapy and meristem culture in apple cultivar 'Oregon Spur-II. Virus Disease 29:75–82. https://doi.org/10.1007/s13337-018-0437-5

Warghane A, Misra P, Bhose S, Biswas KK, Sharma AK, Reddy MK et al (2017a) Development of a simple and rapid reverse transcription-loop mediated isothermal amplification (RT-LAMP) assay for sensitive detection of *Citrus tristeza virus*. J Virol Methods 250:6–10. https://doi.org/10.1016/j.jviromet.2017.09.018

Warghane A, Misra P, Ghosh DK, Shukla PK, Ghosh DK (2017b) Diversity and characterization of *Citrus tristeza virus* and *Candidatus* Liberibacter asiaticus associated with citrus decline in India. Indian Phytopathol 70:359–367

Warghane A, Kokane A, Kokane S, Motghare M, Surwase D, Palchoudhury S et al (2019) Molecular detection and coat protein gene based characterization of *Citrus tristeza virus* prevalent in Sikkim state of India. Indian Phytopathol 73:135–143. https://doi.org/10.1007/s42360-019-00180-3